Pseudocontinuum towards SiO masers: a solution for pointing and focus with non optimal weather conditions at 3 mm

P. de Vicente, A. Pérez, M. Visús, A. Díaz-Pulido

Informe Técnico IT-CDT 2013-01

Revision history

Version	Date	Author	Updates
1.0	25-09-2012	P. de Vicente	First version

Contents

1 Introduction

The 40 m radiotelescope has a low efficiency at 87 GHz (de Vicente 2012, Visús et al. 2012). In order to get a gain curve, do pointing or focus observations, we rely on excellent weather and bright continuum sources. The brightest extra-solar continuum source at the time of this report, is 3C84, with a flux lower than 10 Jy. On the contrary, Mars, Venus, Jupiter and Saturn usually have fluxes larger than 50 Jy and are ideal sources to make an absolute calibration of the telescope. However planets have drawbacks. Jupiter cannot be used at 3 mm since its angular size is larger than the beam. Venus has a variable angular size and, in some ocasions, as with Jupiter, its angular size is larger or comparable to the HPBW of the 40 m dish at 3 mm ($\simeq$ 18 arcsecs), which renders it useless. In some epochs, planets are only visible during the day and close to the Sun. This is a major problem because the radiotelescope reflector structure and the tetrapod suffer large scale deformations during day time which are important when observing above 80 GHz. This makes focusing difficult, generates variability in the amplitude calibration, deforms the beam of the antenna and spoils in some cases the base lines.

This is a non-optimum scenario and we have looked for an alternative to do pointing and focus observations. It is well known since long time ago that strong spectral lines can be used to make these kind of observations. The best fitted lines are the 1–0 and 2–1 rotational transitions of SiO at its first vibrational level, which in many stars appear as masers. This report summarizes observations towards a selected list of stars. Since the maser emission is approximately periodic, with a period between 1 and 3 years, the spectra included in this report will change in the future. In any case, the list provided here is an useful tool for future observations.

2 The effects of weather on the baseline at 3 mm

The 40 m telescope does not have neither a wobbler nor a chopper wheel which allows to make continuum switched observations. This technique consists on fast switching between the source and the blank sky and substracting the emission from both. Usually the blank sky is several HPBWs away from the source to ensure that weather conditions are very similar and that a substraction will remove the contribution from the atmosphere. The fastest the frequency the better the baseline will be. Since switching the beam requires a mechanical movement, this is applied to small mechanical parts with low inertia. Two solutions are available at other telescopes: a moving subreflector (wobbler) or a rotating mirror in front of the ray path which deviates radiation towards the blank sky. In both cases the frequency switch goes from 1 Hz to 10 Hz.

Continuum observations at the 40 m are restricted to total power observations, and require excellent weather. Even under these circumstances the atmosphere changes rapidly and observations are not reliable in some ocasions. Fig. 1 displays two drifts over Venus under different weather conditions to demonstrate how the atmosphere has a strong influence on the baseline.

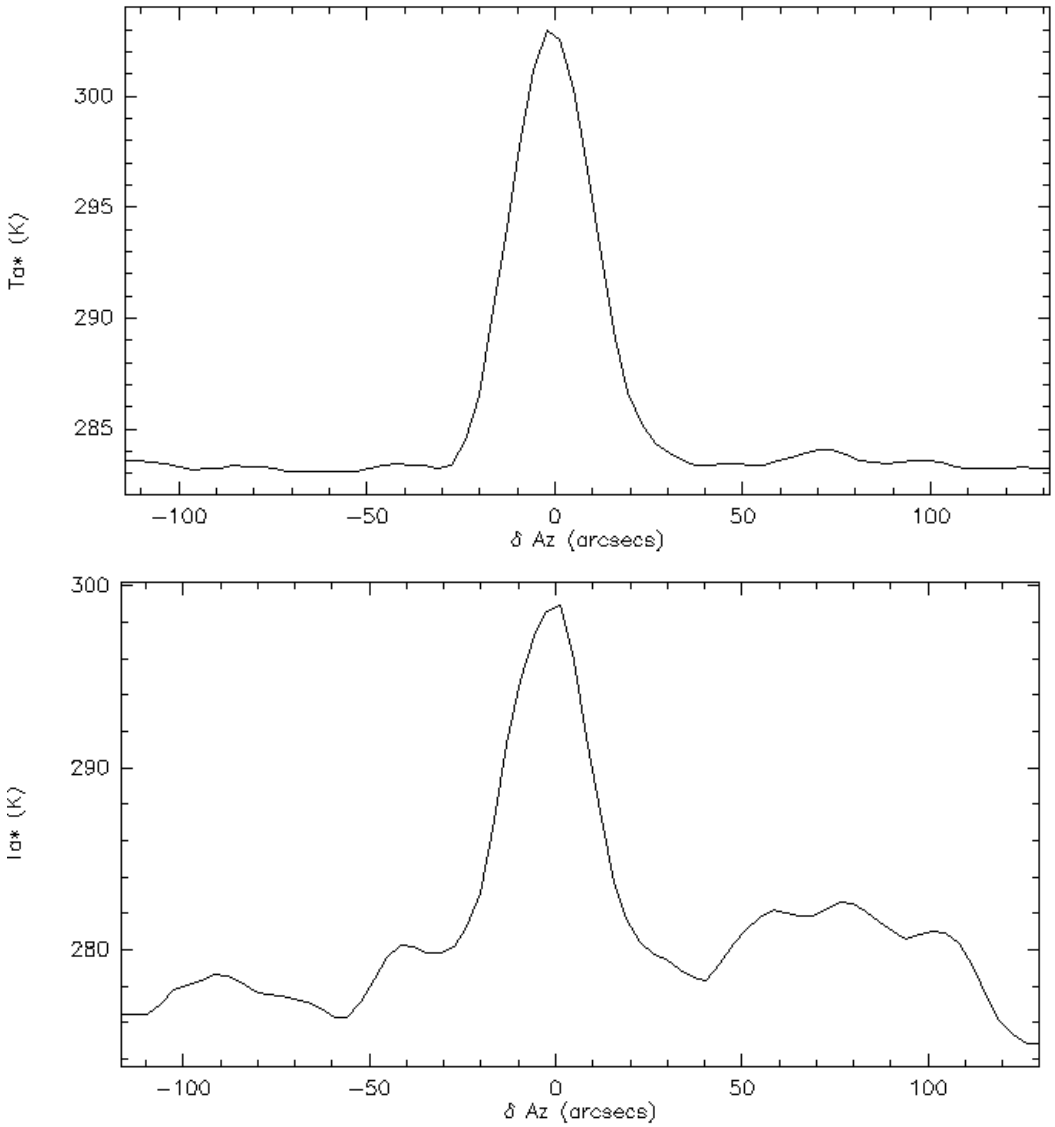

Figure 1: *Total power continuum drift towards Venus at 86 GHz with clear sky (upper panel) and with clouds (lower panel).*

3 The pseudocontinuum

Pseudocontinuum observations consist on making drifts on bright SiO maser sources in the 2–1 rotational transition at the first vibrational state. While making the drift, the FFT backend takes a spectra periodically. The integration time may range between 1 and 3 seconds, depending on the intensity of the masers. The acquisition software, in particular the FitsWriter component, averages the specified frequency channels (where there is emission) and substracts this value from the average of the rest of channels (where no emission is present). Below we include the code that performs the operation to make it clearer:

```
....
unsigned int bsMax = 1;
if (febefeeds == 2) {
   bsMax = 2;
} else {
   bsMax = 1;
}

unsigned int startIndex = 0;

double base = 0.0, peakline = 0.0;
int basecount = 0, peakcount = 0;

if (!pseudocontinuum) {
....
} else {
    for (unsigned int bs = 0; bs<bsMax; bs++) {
       for (unsigned int indexS = 0; indexS < channels; indexS++) {
          if ((indexS > firstchannel) && (indexS < lastchannel)) {
              peakline = peakline + m_fftsvolt[bs][indexS];
              peakcount++;
          } else {
              base = base + m_fftsvolt[bs][indexS];
              basecount++;
          }
       }
       values[bs] = peakline/peakcount - base/basecount;
   }
   // Should be rewritten by next loop
   channels = 1;
}
....
```

In the previous code `firstchannel` and `lastchannel` are the channels that delimit the frequency interval where there is maser emission. `bs` is an integer variable that allows to store the spectra from both polarizations and `bsMax` is the number of available polarizations (1 or 2).

Fig. 2 shows graphically the pseudocontinuum process.

Pseudocontinuum was installed in the 40 m telescope in September 2012 and it may be used for any observing frequency where a maser lines is available. It has been tested for water masers at 22.235 GHz and SiO masers at 86.243 GHz. It should also be available at 43.122 GHz for the SiO 1–0 V=1 rotational transitions when the receiver is installed at the 40 m telescope.

The data are stored in the FITS file as if they were coming from a continuum backend making it completely transparent for all the the pipeline processes afterwards. This kind of osbervation can be done with the 500 MHz bandwidth setup or with the 100 MHz bandwitdh one.

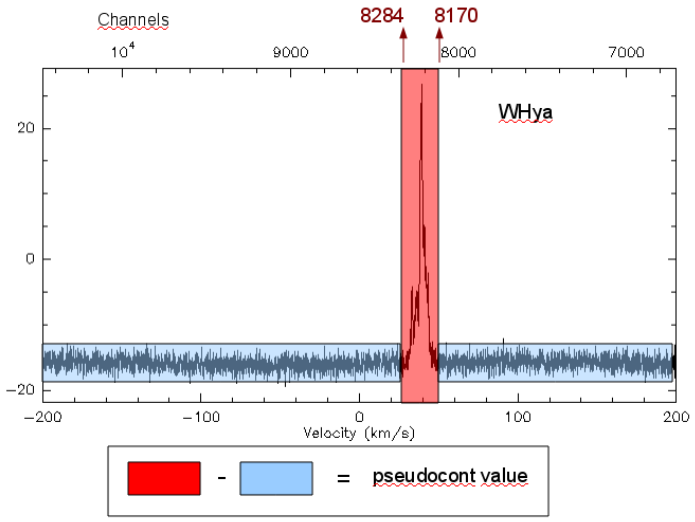

Figure 2: SiO 2–1 v=1 maser emission towards WHya. The red rectangle indicates the frequency interval where channels with emission are averaged. The blue rectangles show the frequency intervals where there is no spectral emission. The figure does not show the whole frequency span of the backend.

The substraction of emission in the frequency domain, in such a small frequency interval (500 MHz at most) and small integration time (maximum of 3 seconds) is very convenient since atmosphere variations are cancelled. This results in very good baselines even under bad weather conditions, with covered sky or irregular distribution of clouds. To test which of the spectral setups gives a higher signal to noise ratio we tested it towards χCyg. Figs. 3 and 4 show the results.

Fig. 3 shows the spectra towards χCyg with the 100 MHz and the 500 MHz bandwdith FFTs backend. Since the number of channels was 16384 for both modes, the spectral resolution is 5 times higher for the former mode than for the latter one.

Fig. 4 shows two pointing drifts with different spectral setups. The left one was done using a 100 MHz total bandwidth and a channel interval for the spectral emission between 8030 and 8306. The right one was done using 500 MHz total bandwidth and a channel interval between 8156 and 8212. The number of channels used for the narrow bandwidth (276 channels) was roughly 5 times those used for the wide band (56 channels). The signal to noise ratio for the 100 MHz and the 500 MHz pseudocontinuum was approximateley 33 and 56 respectively. This means that the wide band spectral setup produces better results than the narrow one. This

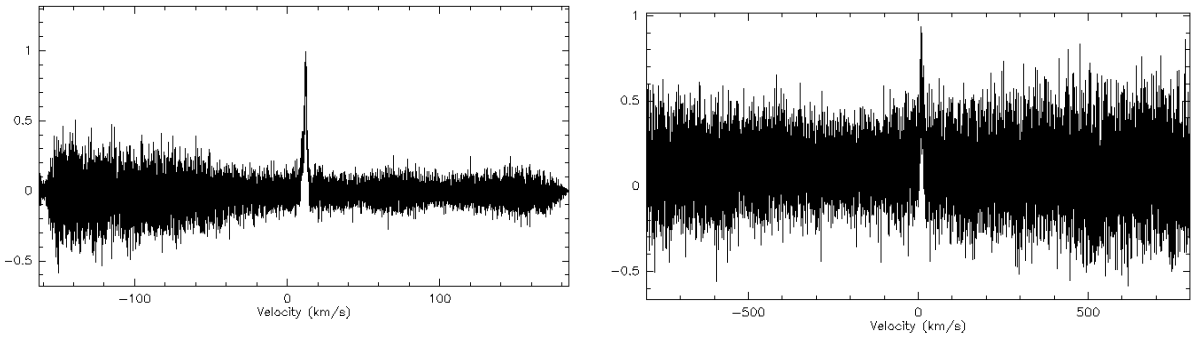

Figure 3: *Spectra towards χCyg at 862243 MHz with a 100 MHz bandwidth (left) and 500 MHz (right). The number of channels was 16384 in both cases. Integration time is 30 seconds*

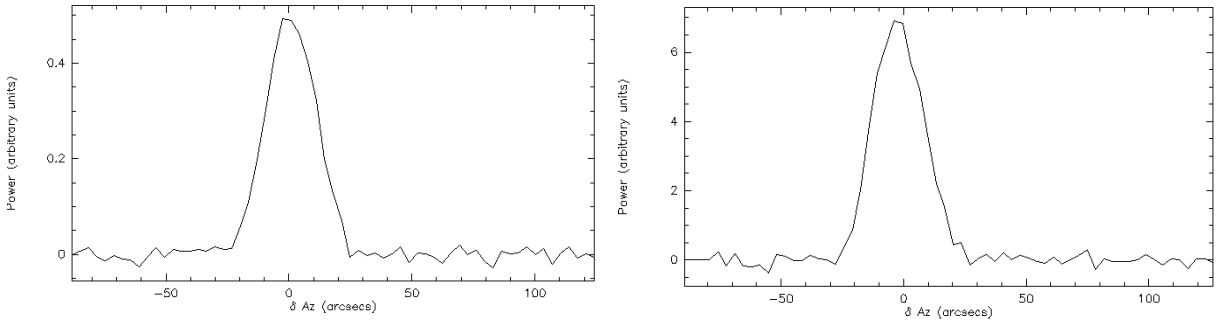

Figure 4: *Pointing drifts towards χCyg at 862243 MHz with a 100 MHz bandwidth (left) and 500 MHz (right). The SNR is 33 in the first case, and 56 in the second one. Apparently higher bandwidth produces better results.*

possibly comes from the fact that the average noise from channels without emission is lower for the wide band than for the narrower one, resulting in a higher SNR after the substraction.

Integration time for pseudocontinuum requires an integration time between 1 and 3 seconds. This value depends on the flux of the source. By default we use integration times of 1 second, however if the antenna temperature of the peak is below XXX? K, the integration time should be 2 seconds and the duration of the pointing scan should be doubled to have the same spatial resolution as in the default case.

4 Observations towards masers

This section summarizes the observations performed between september 13^{th} and 21^{st} and november 9^{th} and 30^{th} towards a selected list of stars with SiO maser emission in the 2–1 rotational transition at the first vibrationa level (V=1). Table 4 summarizes the most important parameters: coordinates, maximum T_a^*, channels used to do pseudcontinuum observtaions for both the 500 MHz bandwidth and the 100 MHz bandwitdh spectral setup, velocity of the LSR and the date of the last observation and to which the previous parameters refer to.

All observations were done using the Fast Fourier Spectrometer with 16384 channels and either with a maximum bandwidth of 500 MHz or 100 MHz. Scans were of the spatial ON - OFF type, where the OFF positions, used as reference, were 200 arcsecs apart in azimuth and at the same elevation to ensure that the atmosphere had the same contribution as the ON subscan. In millimeter observations the atmosphere emission strongly depends on the elevation. All scans were composed of 30 seconds integration time subscans. The FFTS was configured to use a dump integration time of 5 seconds, except in some cases where 1 second dump integration time was used. This is marked in table 4

4.1 Source's spectra ordered by RA

In this subsection we include the spectra of all stars at 86.4 GHz, which correspond to the SiO 2–1 V=1 rotational transition at the date specified in Table 4. Since the spectral features are narrow and to allow a better view we only show a restricted velocity interval of 100 km/s around the peak temperature. All spectra are included with their CLASS full headers to help the reader identify the main observation parameters.

Source	**RA** J2000	**Dec** J2000	$\mathbf{T}_a^*$ (K)	**Channels** (500 MHz)	**Vlsr** (km/s)	**Date**
OMICET	02:19:20.79	-02:58:39.49	48.5	[7280,7325]	+47	Jan-13
IKTAU	03:53:28.87	11:24:21.70	30	[8156,8260]	+34	Jan-13
TXCAM	05:00:50.39	56:10:52.60	130	[8297,8410]	+24	Jan-13
OriIrc2	05:35:14.49	-05:22:29.30	88	[7952,8303]	+0	Jan-13
UORI	05:55:49.17	20:10:30.69	7.5	[8342,8365]	-40	Nov-12
VYCMA	07:22:58.33	-25:46:03.23	50	[7948,8380]	+20	Jan-13
RCNC	08:16:33.83	11:43:34.46	3	[8401,8464]	35	Nov-12
XHYA	09:35:30.26	-14:41:28.60	< 0.66		+26	Jan-13
RLEO	09:47:33.49	11:25:43.66	25	[8123,8227]	-1	Nov-12
RLMI	09:45:32.28	34:30:42.77	5	[8223,8309]	+10	Jan-13
RTVIR	13:02:37.98	05:11:08.38	4.8	[8137,8261]	+18	Jan-13
RHYA	13:29:42.78	-23:16:52.77	< 0.53		-9	Nov-12
WHYA	13:49:03.00	-28:22:03.49	69	[8170,8284]	+42	Nov-12
RXBOO	14:24:11.63	25:42:13.41	3.5	[8130,8228]	+1	Nov-12
S CrB	15:21:23.96	31:22:02.57	10	[8084,8169]	-5	Jan-13
R Ser	15:50:41.73	15:08:01.10	2.5	[8113,8163]	+37	Nov-12
RUHER	16:10:14.5	25:04:14.33	3.5	[8317,8239]	-13	Nov-12
UHER	16:25:47.47	18:53:32.85	12	[8054,8138]	-15	Jan-13
VXSGR	18:08:04.05	-22:13:26.63	7.5	[8152,8291]	8	Jan-13
V111OPH	18:37:19.26	10:25:42.20	6	[8446,8507]	0	Nov-12
RAQL	19:06:22.25	08:13:48.01	20	[8177,8224]	+48	Nov-12
chiCyg	19:50:33.92	32:54:50.61	30	[8156,8212]	+11	Nov-12
GYAQL	19:50:06.33	-07:36:52.49	10	[8166,8189]	+34	Nov-12
NMLCYG	20:46:25.54	40:06:59.40	3.6	[8090,8376]	-1	Jan-13
UX Cyg	20 55 05.52	30:24:52.10	< 1.87		-3	Jan-13
TCEP	21:09:31.78	68:29:27.20	8.2	[8178,8248]	-1	Jan-13
MUCEP	21:43:30.46	58:46:48.16	25	[7908,7968]	+0	Jan-13
RS Peg	22:12:16.18	14:33:12.24	< 2.45		-20	Jan-13
W Peg	23:19:50.5	26:16:43.66	6.7	[8118,8186]	-21	Jan-13
LPAnd	23:34:27.53	43:33:01.20	< 3.27		-18	Jan-13
RAQR	23:43:49.46	-15:17:04.14	5.5	[8330,8459]	-28	Jan-13
RCAS	23:58:24.87	51:23:19.70	168	[7706,7765]	-23	Nov-12

Table 1: T_a^* corresponds to the brightest spectral feature

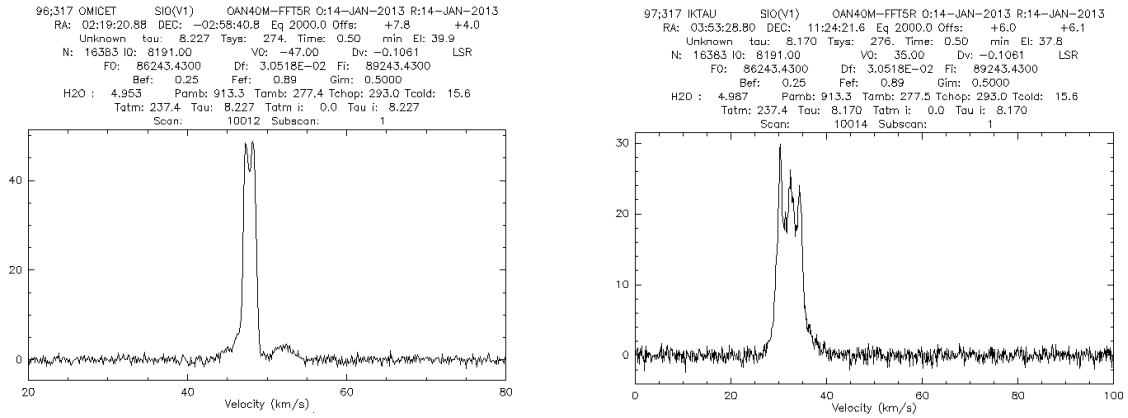

Figure 5: *Left: Omicet. Right: IkTau.*

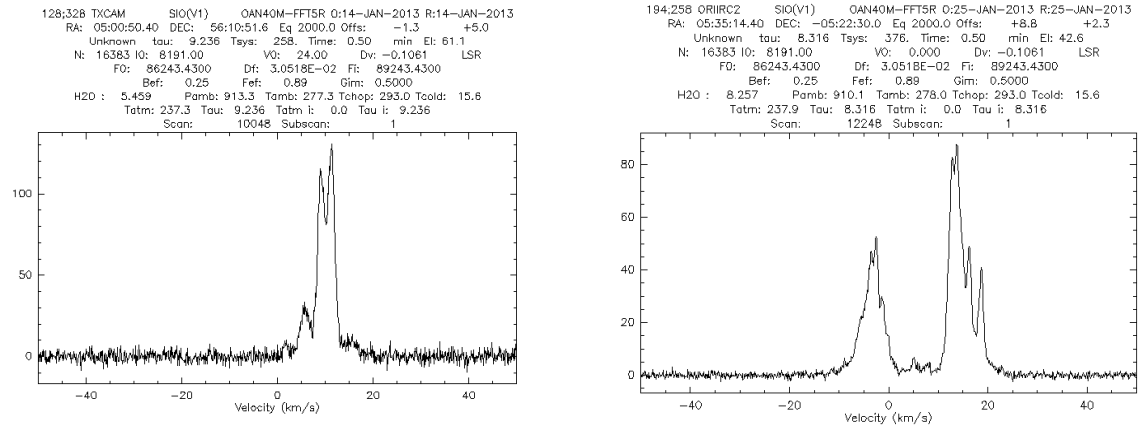

Figure 6: *Left: TXCam. Right: OriA.*

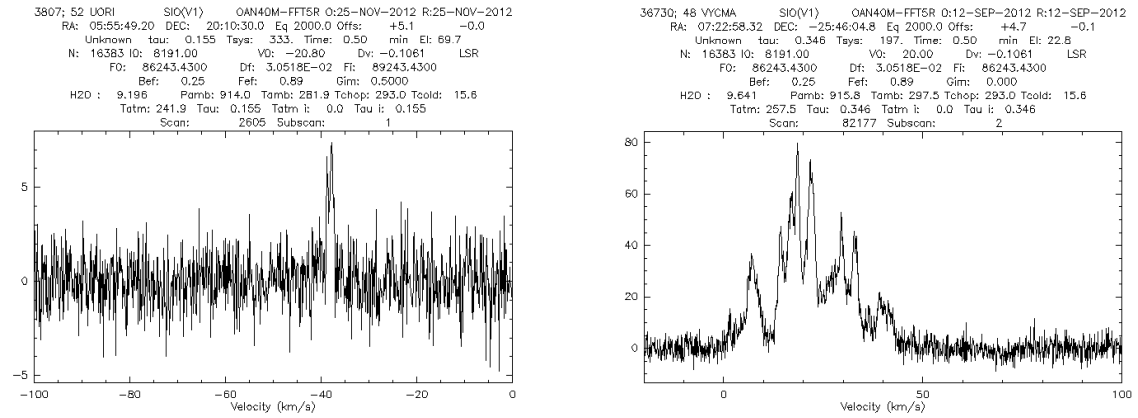

Figure 7: *Left: U Ori. Right: VYCma.*

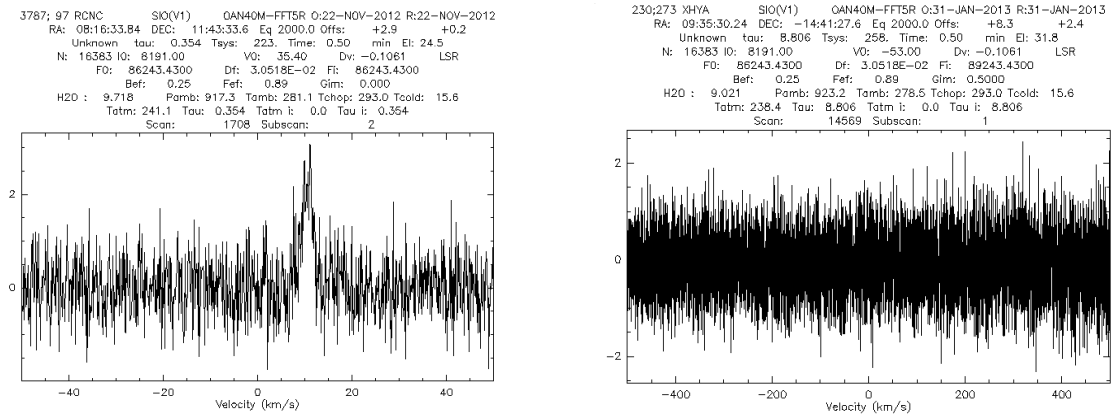

Figure 8: *Left: R Cnc. Right: XHya.*

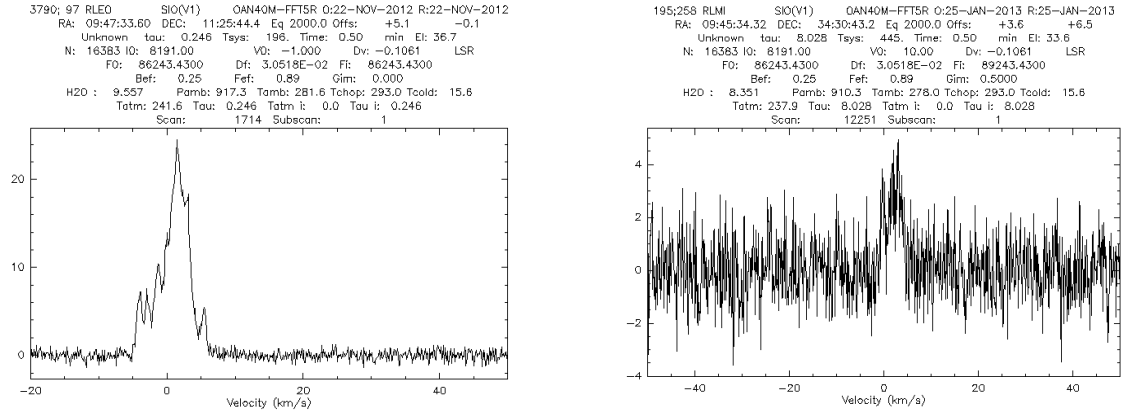

Figure 9: *Left: R Leo. Right: RLMI.*

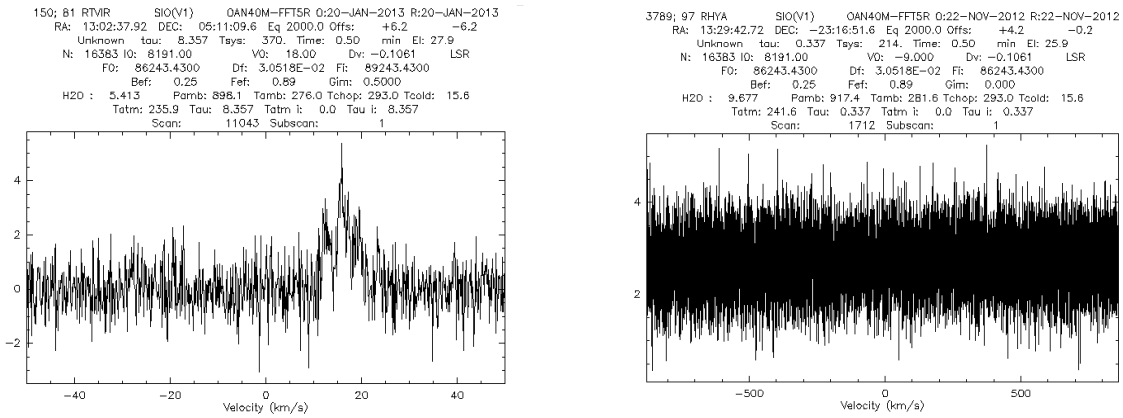

Figure 10: *Left: RTVir. Right: R Hya.*

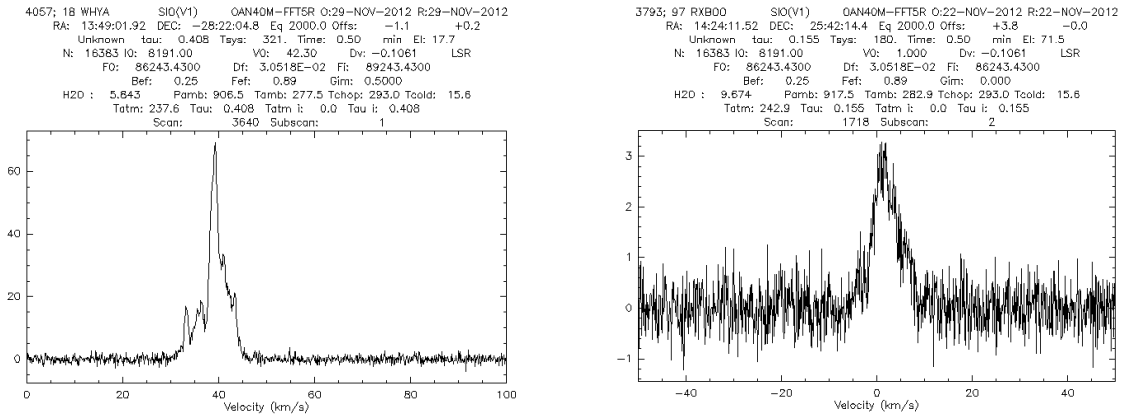

Figure 11: *Left: W Hya. Right: RXBoo.*

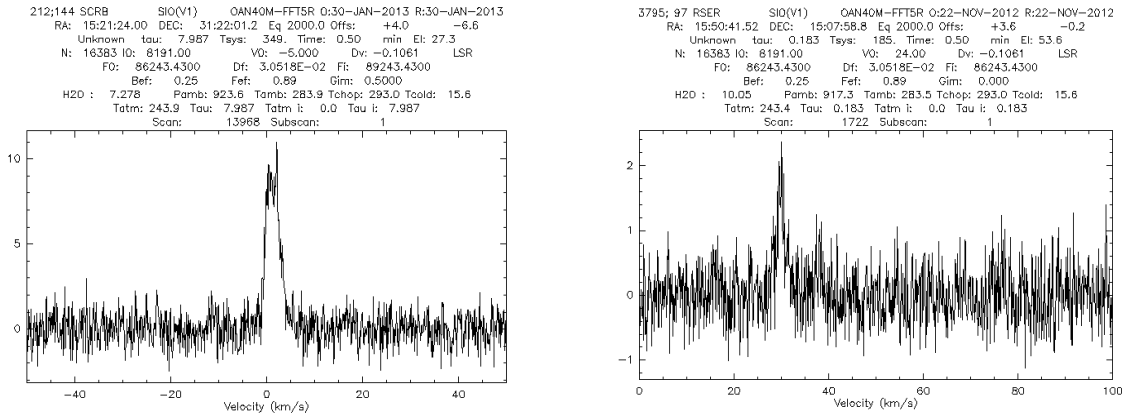

Figure 12: *Left: S Crb. Right: R Ser.*

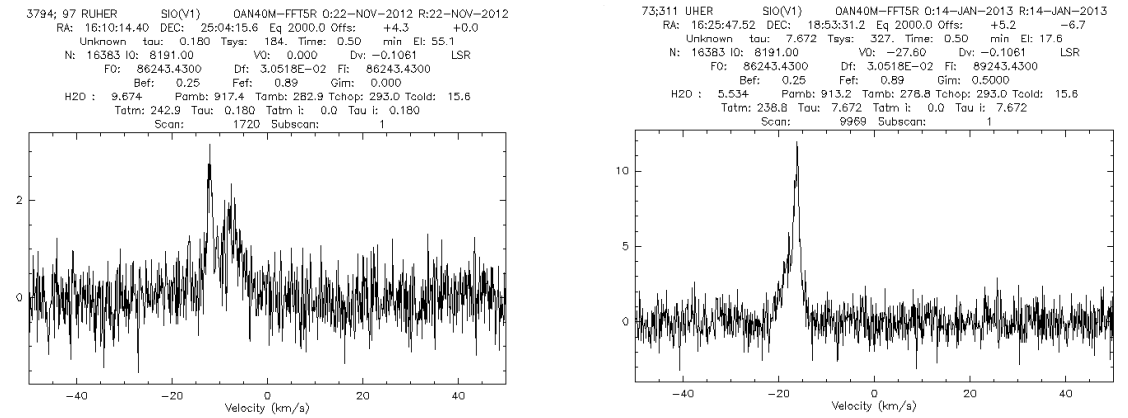

Figure 13: *Left: Ru Her. Right: U Her.*

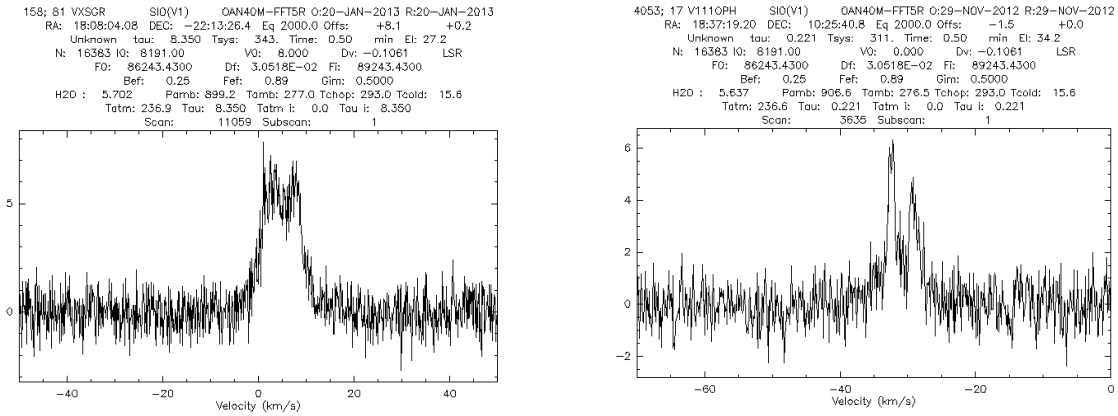

Figure 14: *Left: Vx Sgr. Right: V111Oph.*

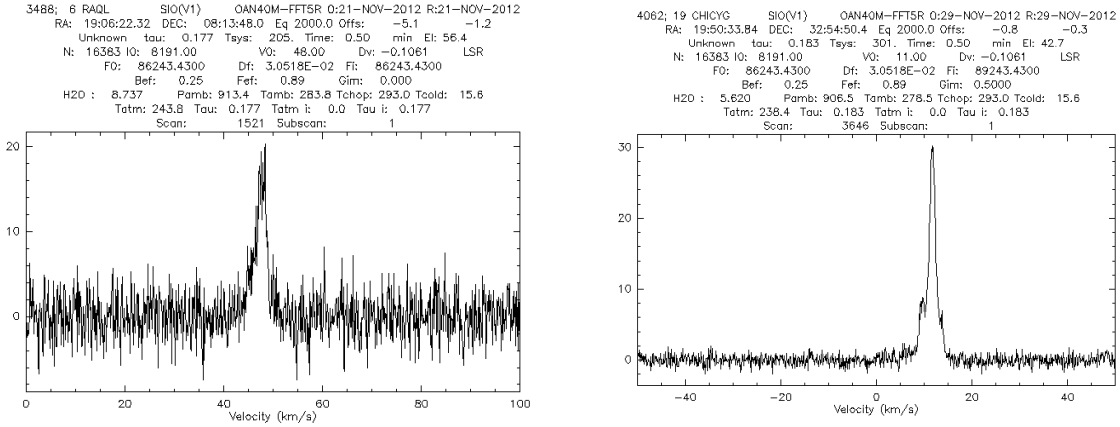

Figure 15: *Left: R Aql. Right: Chi Cyg.*

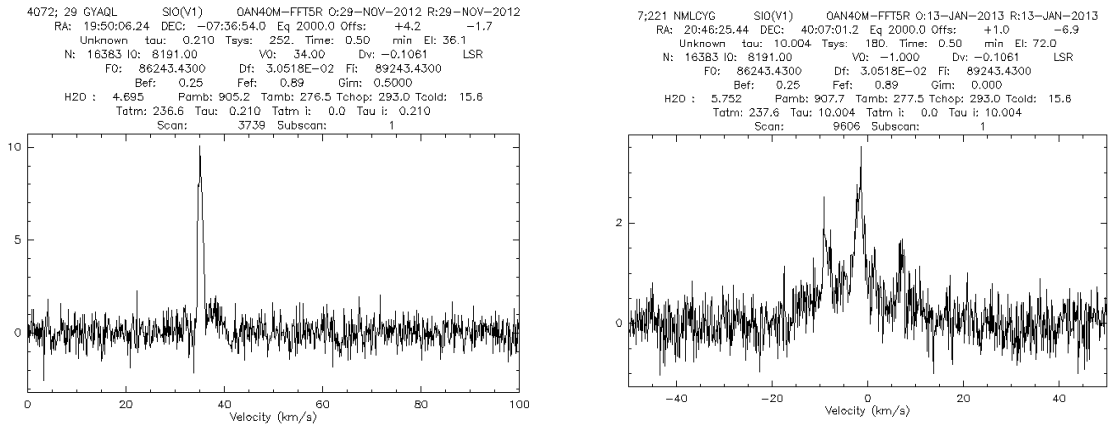

Figure 16: *Left: Gy Aql. Right: NML Cyg.*

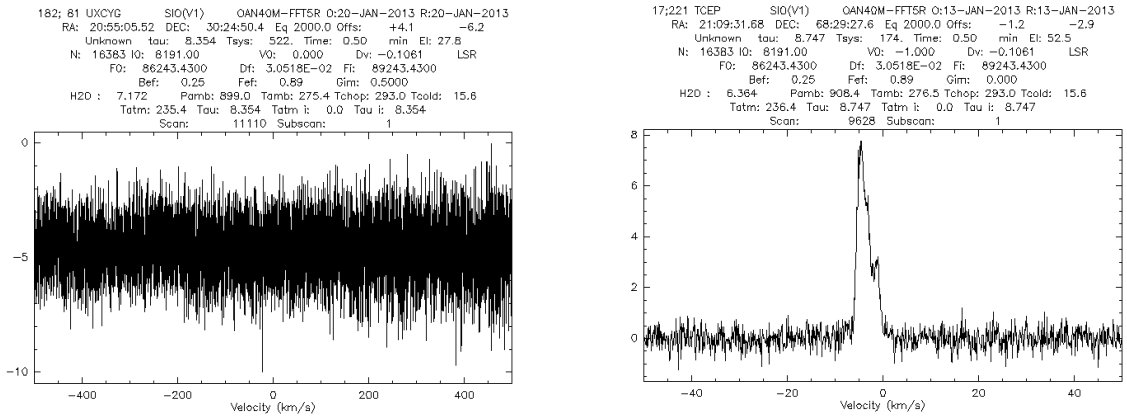

Figure 17: *Left: Ux Cyg. Right: T Cep.*

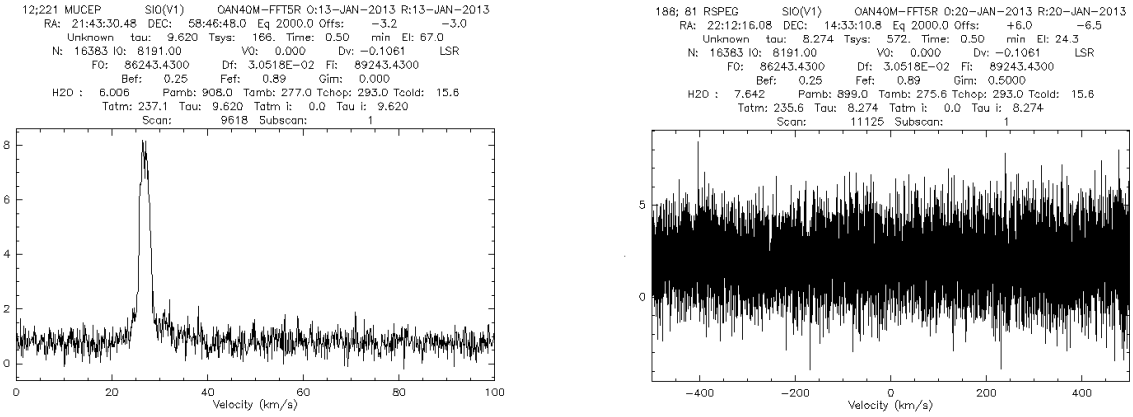

Figure 18: *Left: Mu Cep. Right: Rs Peg.*

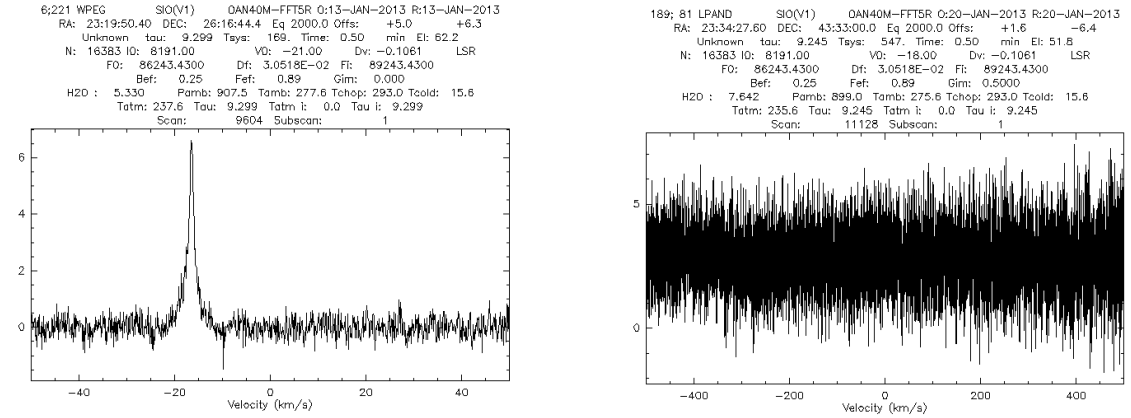

Figure 19: *Left: W Peg. Right: Lp And.*

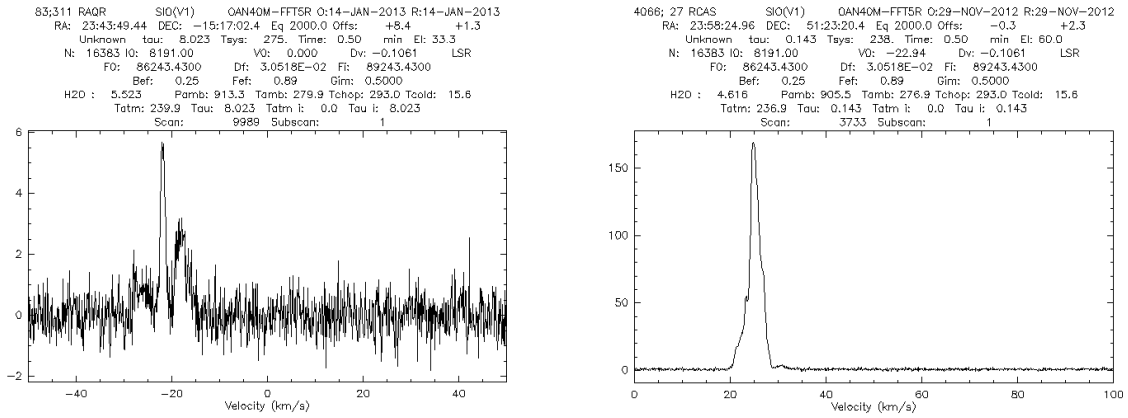

Figure 20: *Left: R Aqr. Right: R Cas.*

5 Criteria to select pseudcontinuum drifts

Fig. 21 displays 3 pseudocontinuum drifts with different signal to noise ratios. Based on such plots we have adopted the criteria that drifts will be considered reliable and useful when its SNR is above 15.

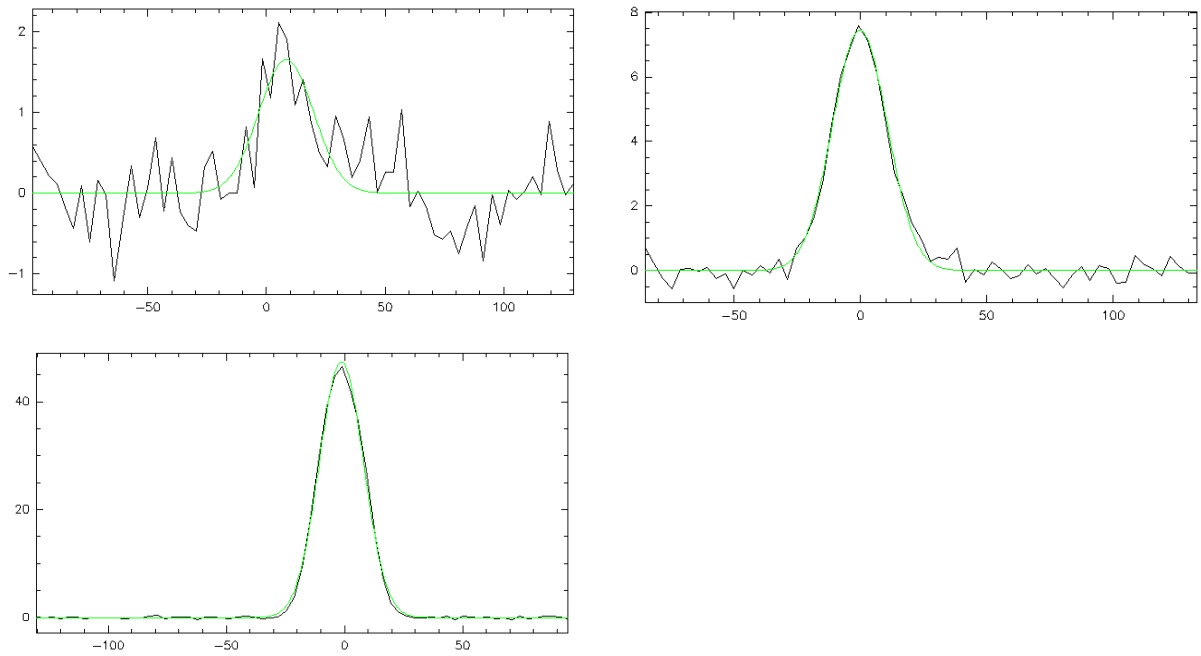

Figure 21: *Pseudocontinuum drifts with different SNRs. Upper left: SNR∼3 (UOri), upper right: SNR∼28 (TXCam), lower left: SNR∼193 (RCas)*

Fig. 22 displays the signal to noise ratio (SNR) versus the product of the maximum antenna temperature times the number of channels for pseudocontinuum drifts for a selected sample of 12 sources. The SNR depends approximately on the square root of the product.

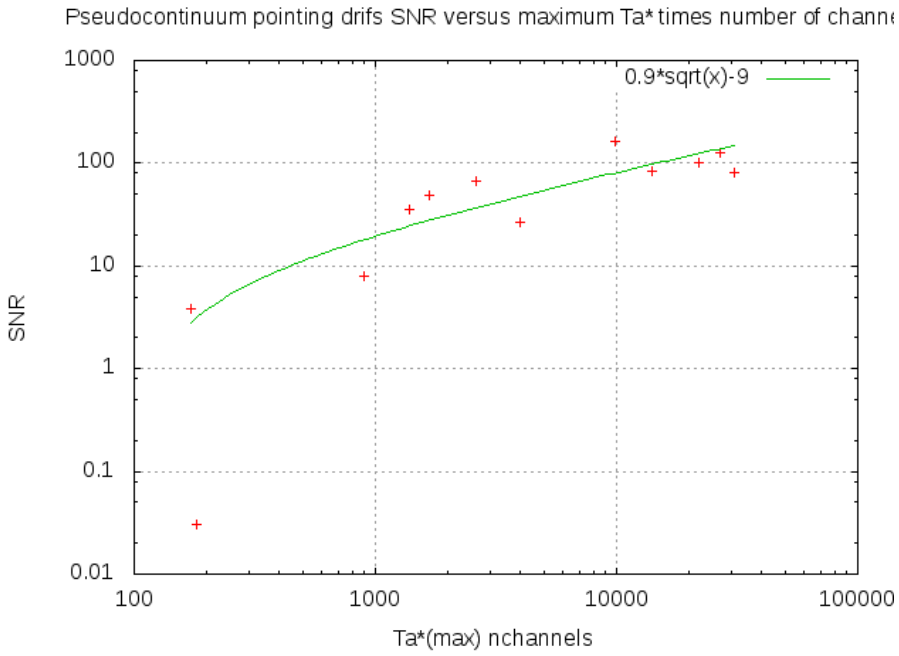

Figure 22: *Signal to noise ratio for 12 sources versus the product of the maximum antenna temperature times the number of channels of the emission (the spectral resolution of each channel is 30 KHz)*

6 Variability of the SiO maser sources

Most of the SiO masers arise around pulsating stars. Its emission flux is variable and heavily depends on the conditions of the central star. Therefore pseudocontinuum observations that rely on variable masers require a regular monitoring of the sources. The 40 m will make this monitoring probably twice per year in its procedure to check for pointing and focus. In any case a good starting point is to look up the light curve of the stars in the AAVSO web page (`http://www.aavso.org/lcg`. It is known that there is a good correlation between the SiO maser activity of variable stars and their near and mid-IR emission, which lags about 0.1 to 0.2 from its optical phase (Bujarrabal et al. 1993).

Fig. 23 shows the light curve of χCyg from the AAVSO web page for an interval of 600 days. This kind of plots are an excellent tool to estimate if some sources are good candidates for pseudocontinuum observations.

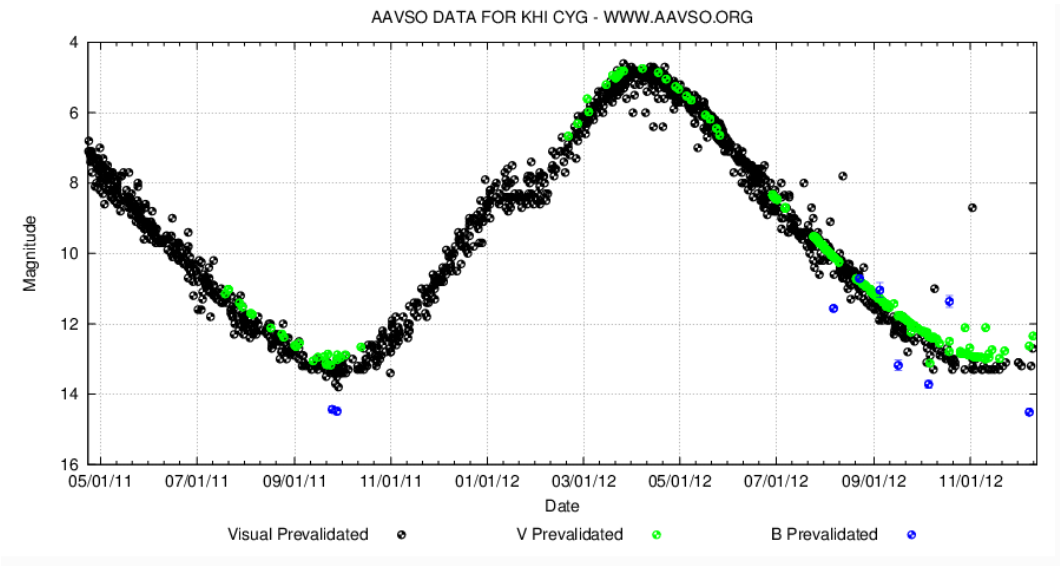

Figure 23: *Light curve for χCyg at the V and B bands obtained from the AAVSO web page.*

References

[Bujarrabal 1993] V. Bujarrabal, J. Alcolea, A. Martínez, A. Barcia, J. D. Gallego, J. Gómez-González, A. del Pino, P. Planesas, R. Bachiller, A. Rodríguez, A. del Romero, M. Tafalla, P. de Vicente. Lecture Notes in Physics Volume 412, 1993, pp 421-424.

[de Vicente 2012] P. de Vicente. The 40m radiotelescope at the 87-110 GHz band after holography. IT OAN 2012-09.

[Visus 2012] M. Visús, P. de Vicente, A. Pérez, V. Bujarrabal, A. Díaz-Pulido. Aperture Efficiency and Astigmatism Measurements at 87-110 GHz. IT OAN 2012-20.